

Investigation of Branching in Polycarbonate due to Stress Corrosion

Ulf Hejman^{1, a} and Christina Bjerken^{1, b}

¹Div. material science, Malmö University, SE-205 06, Sweden

^aulf.hejman@mah.se, ^bchristina.bjerken@mah.se

Keywords: crack branching, stress corrosion, chemically assisted crack growth.

Abstract. In this study, experiments have been made to investigate how the width of stress corrosion cracks change when branching occurs. The amount of dissolved material is investigated using an optical microscope. Crack width before and after branching and characteristic crack angles are measured. It was found that the total width of the branches is preserved after branching and a connection to the stress intensity factor at the crack tips is suggested. It is assumed that quasi-static calculations for branched cracks, found in literature, can be applied to these cracks. Experiments have been performed on polycarbonate with acetone as a dissolving agent. Experimental results are compared with numerically simulated results as well as with data found in literature.

Introduction

Stress corrosion is a common problem in engineering constructions. Stress corrosion can cause failure well under the yield stress of the material. Three prerequisites, namely a susceptible material, a corrosive environment and mechanical stress have been identified for stress corrosion. Metals are often listed together with their corresponding corrosive environment. Such a list of metals and environments combinations that exhibit stress corrosion cracking is found in e.g. Davis [1] and a general description of the phenomena can be found in e.g. Jones [2]. Also ceramics and polymers exhibit stress corrosion. A transparent thermoplastic polymer that is the object of this study is polycarbonate. Fig. 1 a) shows a typical stress corrosion crack from the experiments.

A stress corrosion crack is different from a sharp crack driven by mechanical load alone since they can branch. There are two different kinds of stress corrosion. Brittle fracture can arise from uptake of hydrogen, a phenomenon known as hydrogen embrittlement. Stress corrosion cracks can also form from dissolution of material. In this case, they have a finite width and the crack tip is blunt even in the absence of load or plastic deformation, cf. Jivkov [3]. The stress corrosion cracks in metals are due to dissolution and transformation to an oxide. Many polymers sensitive to stress corrosion, e.g. polycarbonate used in this study, are also examples of stress corrosion due to dissolution.

Most research, in the field of stress corrosion, has been done to experimentally measure crack propagation rates for both statically loaded specimens and for cyclic loading, cf. [2]. Lifetime predictions and evaluation of different material and environment combination are the most common interests. In all these studies the failure is considered. In this study, the nature of the branching and the stress intensity factor at the crack tip before and after branching is investigated. An experiment is performed and the geometrical characteristics of repeatedly occurring branching are studied. A correlation of the ratio of the stress intensity factor at the cracks tips and the crack widths before and after branching is studied. The experimental results are also compared with a numerical method to simulate stress corrosion cracks. The method is based on a moving boundary formulation for a finite element method developed by Jivkov and Ståhle in [3,4].

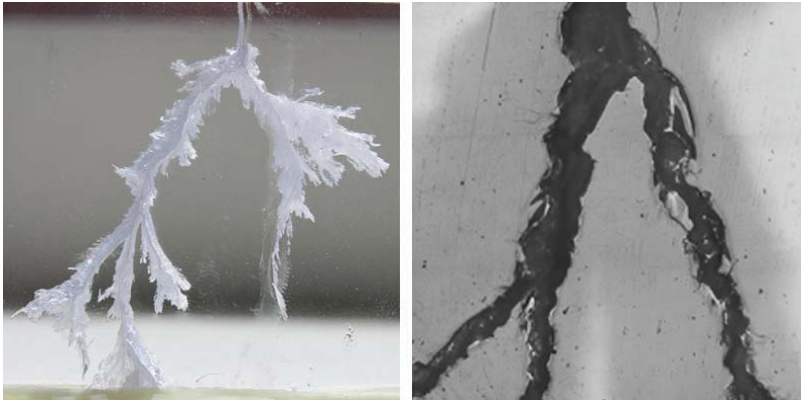


Figure 1 a) Stress corrosion crack in polycarbonate. b) A Crack branch in polycarbonate

General description of the analysis

Stress corrosion cracks have a characteristic appearance and can easily be distinguished from other cracks due to the many branches. Branches are normally associated with dynamic crack growth, but stress corrosion cracks grow at speed much below the speed of sound for the material. Fig. 1 b) shows a stress corrosion crack in the polycarbonate, used in this investigation. From the figure, it can also be seen that the stress corrosion crack have a finite width that decreases after each crack branch. In this study a correlation between the crack width and the stress intensity factor at the crack tips is investigated.

It is known that cracks are prone to follow a mode I path, cf. Broberg [5]. This behaviour is observed to be independent of the crack growth mechanism, virtually without exceptions. There are a number of calculations made for sharp cracks that have branched and many of them assume mode I crack growth. The usual aim is to calculate dynamic crack growth using quasi-static stress state. These crack configurations can be applied to stress corrosion cracks which are assumed to grow under quasi-static conditions to get approximate values of the stress intensity factor at the branch crack tips. The mode I stress intensity factor, K_I , for branched sharp cracks have been calculated for various crack branch configurations. Analytical as well as numerical methods have been proposed by, e.g. Pärletun [6], Vitec [8], Zhang [8], Suresh [9] for mode I and by Theocaris [10,11] for mixed mode loading. For symmetric crack branching with equally long crack branches Pärletun [7] have calculated the most favourable crack dividing angle to 26° , and the stress intensity factor decreases by a factor 0.7 for the branches compared to the stress intensity factor before branching. Other researchers [7-11] report similar results.

For small scale yielding, the following relation exists between the stress intensity factor and the J -integral

$$J = \frac{K_I^2}{E} \quad (1)$$

where E is the material's elastic modulus. When the crack branches, it is fair to assume that the J -integral is, at least initially, unchanged. If this is the case, the sum of the two branches J -integrals, J_1

and J_2 , where 1 and 2 indexes the two branches of the crack, will be equal to the J -integral according to

$$J = J_1 + J_2 \quad (2)$$

and this gives a relation for the sum of the stress intensity factors

$$K_I^2 = K_{I1}^2 + K_{I2}^2 \quad (3)$$

The above equation is also derived by e.g. Suresh and Shih [10] in a more rigorous way. If the stress intensity factor decreases by a factor approximately 0.7, or slightly above, for the two branches, as reported from for example e.g. Pärletun [6], Suresh and Shih [9], Theocaris [10-12]. It is fair to estimate this numerical result with $1/\sqrt{2}$ for symmetrically branched cracks. This is in line with Eqs. (2) and (3) that shows that the energy scales linearly for the two branches whereas the crack intensity factor scales with the square.

The sudden change of stress intensity factor after branching affects the state of the crack growth. Early investigations indicated that, for sharp cracks, the decreased stress intensity factor lead to a decrease in crack propagation rate. It was, however, reported by Carter [13] that this could not be the case for stress corrosion cracks. The crack growth rate is initially linearly dependent on the stress, but reaches a plateau where it is constant and insensitive to the load. Carter also states that there must be a threshold value for crack branching. It was later shown theoretically by e.g. Stähle et al. [14] that the propagation rate can be independent of the load. A drop in the stress intensity factor instead affects the crack width. The following model from Jivkov [3,4] and Stähle [14] is adopted to describe the connection between the strains at the crack tip and the amount of dissolved material, and thus the width of the crack. In the numerical model, dissolution is assumed to take place at the surface where the strain exceeds a threshold value. When the stress intensity factor decreases, the strains at the crack tip decreases and a smaller area at the crack tip is dissolved. In the present study the correlation of the stress intensity factor to the crack branch widths before and after branching is investigated.

Material

The material used in this investigation is an industrial-grade of MACROCLEAR polycarbonate (Arla plast), which is a transparent thermoelastic polymer with Young's modulus $E=2.3$ GPa and tensile yield stress $\sigma_y=63$ GPa. In this study, all specimens were cut in the same direction, parallel to the machining direction, and no investigation was made for different directions in the material. Acetone is used as a dissolving agent. It diffuses easily in polycarbonate and dissolves it in a hydrolysis process that is comparably fast which is attractive when a large number of experiments are made. Ghorbel [17] have shown that static stresses in the polycarbonate drastically accelerate the hydrolysis. The growing crack may easily be followed by the naked eye. It is assumed that inertia effects are insignificant.

Specimen

The polycarbonate plate was cut out from a sheet with the thickness $t = 10$ mm thick sheet. The cutting was done using a hacksaw and the edges were polished to a reasonable smoothness. The dimensions are shown in Fig. 2, where the width $w = 10t$ and the height $h = w/2$ where t is the thickness $t=10$ mm. A coordinate system is attached to one of the corners of the plate as shown in Fig. 2, so that the plate covers the region $0 \leq x \leq w$ and $0 \leq y \leq h$ in the x, y plane. A very stiff support was created along the boundary $y=0, 0 \leq x \leq w$ by an aluminium bar that was glued on the

plate using epoxy glue supplied by Plastic Padding. A small notch was made perpendicular to the opposed edge at $x = w/2$ and $h - a_0 \leq y \leq h$, where the initial length of the notch, a_0 , is approximately $h/5$. The notch was made with a hacksaw giving it the initial width of $t/10$. Two holes with the diameter of 3 mm, were drilled through the plate on each side of the notch at a distance $a_0/2$. Fig. 2 shows the approximate position of the holes. The holes were used to apply a load to the specimen.

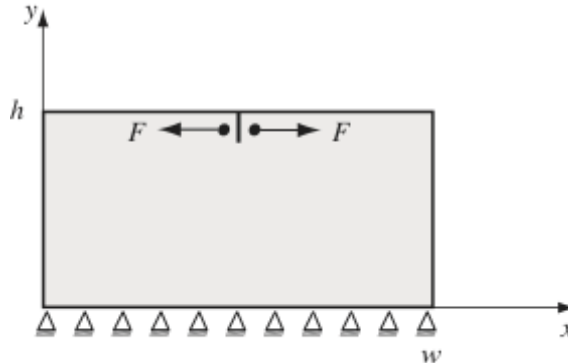


Figure 2. Geometry, boundary conditions and loading of the specimen.

Experimental setup

An even and continuous flow of acetone to the crack tip was obtained by adding acetone by a small paper strip introduced between the edges of the notch. Two opposed forces F were applied in the x -direction to each of the holes in the plate, as Fig. 2 shows.

The crack branches in the cracked specimen were photographed with an optical microscope. Because of the plastic deformation, the crack will not close when the load is removed. A method was developed to account for this effect and remove the parallax from the images of the specimen's surface so that only the crack width due to dissolution could be determined. The sides of the specimen were lightly scratched with fine sandpaper before the load was applied. These scratches were used to match the crack sides to each other with help of an imaging software. By matching the sides of the crack to make them fit together with continuous scratches passing across them, the dissolved part could be identified. The procedure is shown in Fig. 3.

Since the crack branches repeatedly, a large number of branches could be analysed in each specimen. All branching points in this investigation are treated equally.

The model

The evolution of a stress corrosion crack is modelled as a moving boundary problem, where the material is assumed to dissolve at locations along crack surface that experience large strains. A geometry corresponding to the experiments is used in the simulations. Plane strain is assumed to prevail. This corresponds to an infinitely thick plate and the assumption ought not to influence the relative relations between the characteristics of branching that are investigated in the present study. For the simulations of crack growth, a linear relation between the surface strain ε and the dissolution rate v is assumed

$$v = C(\varepsilon - \varepsilon_{th}) \quad \text{for } \varepsilon > \varepsilon_{th} \quad (4)$$

where C is a constant depending on the chemical and mechanical properties of the environment and the material. The surface is moved according to Eq. 4 along the normal direction to the surface. The width of the crack may vary during growth, but the crack tip will always be blunted due to the dissolution process. An adaptive finite element procedure was used for the simulations. For further details see, cf. Jivkov [3,4].

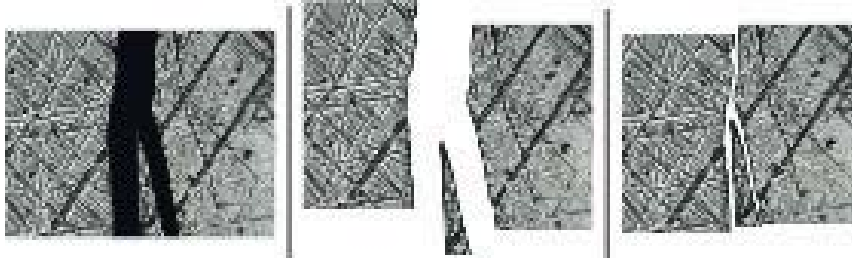


Figure 3. Fitting of the cracked surface to eliminate rigid body motion.

Crack width measurements

Fig. 4 shows how the measured crack branch widths and crack angles are defined. L is the width of the crack just before branching. l_1 and l_2 are the widths of the two branches, where l_1 is always chosen as the widest branch. α is referred to as the crack kink angle, and is always measured to the widest crack branch. The angle between the two crack branches is called the crack-dividing angle and is denoted β . The sum $\alpha + \beta/2$ is defined as the average crack path. This means that if the crack branches symmetrically, the average crack path would continue in the same direction as the original crack and if the crack branch is asymmetrical, the average crack path would turn in the direction of the crack branch that diverges the most. The average crack path is shown in Fig. 4 by a dashed line

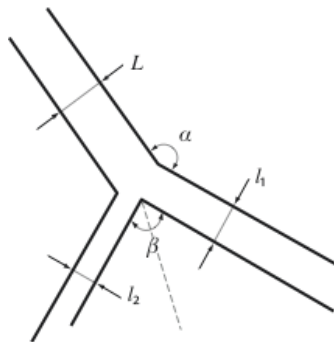


Figure 4. Definition of the crack widths and angels.

To verify the assumption that the stress intensity factor governs the dissolution of material and thereby determines the width of the crack, the non-dimensional sum of the widths after a crack branch $(l_1 + l_2)/L$ was plotted versus the ratio of the widths after branching, l_1/l_2 . In Fig. 5, the ratio $(l_1 + l_2)/L$ is equal to unity when the sum of the two branches is equal to the width before. If the dissolution of material at the crack tip during crack growth is controlled by the mode I stress intensity factor, this is an expected result as discussed previously.

It is seen that the sum of the widths of the crack branches versus the width of the original crack before branching is slightly larger than unity for both the experiments and the simulations. This indicates that, although the stress intensity factor drops, it will, as an average, not drop fully by $1/\sqrt{2}$ but rather be somewhat larger. This result also agrees well with Pärletun [6], Suresh [9], Theocaris [10,11] and Kitagawa [16], who report a stress intensity factor that is slightly larger than 0.72.

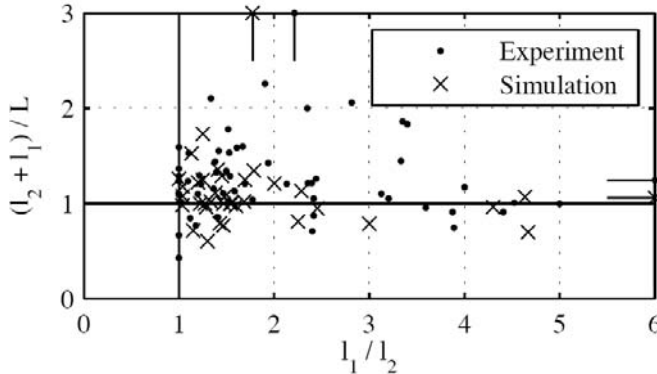


Figure 5. The sum of the widths of the branches versus the ratio of the widest and the most narrow crack.

For symmetry reasons, the cracks could be expected to divide into two equally wide cracks, and although many cracks do, the scatter is large and there is a clear tendency that the cracks form one larger branch, and one smaller branch. Despite the fact that the latter crack is smaller than the other, it will continue to propagate. This phenomenon is typical for stress corrosion crack growth but is not expected from sharp cracks driven only from stress, since the longer crack shades the smaller and decreases the crack tip driving force of the smaller crack.

Crack angles measurements

Both the crack kink angle α and the crack-dividing angle β are measured, and the average crack path, $\alpha + \beta/2$, as measured from the experiments and simulations are shown in Fig. 6. The average values are also indicated in the figure. For the experiments, the average value is $\alpha = 176^\circ$ and for the simulations it is $\beta = 192^\circ$. Both values are determined with a standard deviation of 12° . Also, an immediate glance at Fig. 6 a) and b) shows that it is difficult to distinguish between the experimental and the simulated results. The average values indicate that experimental cracks tend to bend inwards and collect the branches together ($\alpha + \beta/2 < 180^\circ$), but the simulated cracks bend outwards in a more disseminated manner ($\alpha + \beta/2 > 180^\circ$), however, the deviation from 180° is not significantly large.

Cracks that do not branch symmetrically are also expected to be asymmetrical in their widths. Fig. 6 a) shows the sum of $\alpha + \beta/2$ vs. the ratios of the crack widths after branching. All results are collected around the average crack path equal to 180° , and the largest ratio of the crack branch widths is approximately 5 for the experiments and 4.6 for the simulations. The average angle from the experiments and simulations is also indicated in the Fig. 6 a). From the experimental data, it is hard to find any correlation between the width ratio and average crack path. Even for l_1/l_2 ratios up to 5, there are data points in the same range as it is for smaller ratios. This can be interpreted that the main branch continues rather straight forward while the smaller one diverges.

Figure 6 b) shows the distribution of found average crack paths. It is again seen that most cracks continue forward but the experimental results give an average crack path somewhat smaller compared to what the simulation give.

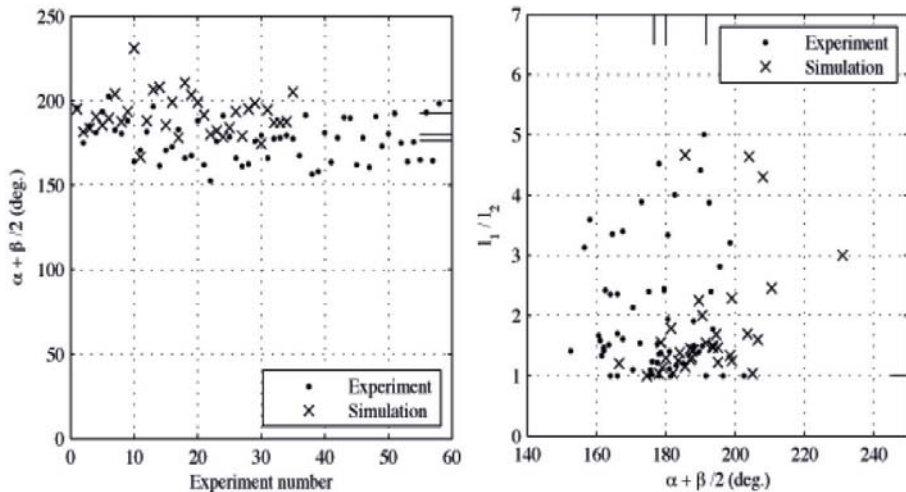


Figure 6 a) The average crack path for the experiments. b) The average crack path versus the ratio of the widths of the branches. In both figures the average values are indicated.

This observations lead to the conclusion that most cracks branch symmetrically with small l_1/l_2 ratios, but with some scatter in the resulting main crack path. Equally wide branches do not always lead to a symmetric crack branch. All measurements of the average crack path is in the interval 155° - 215° .

The individual measurements of the α and β angles is shown in Fig. 7. The average values were found to be $\alpha=161^\circ$ for the experiments and $\alpha=168^\circ$ for the simulations and $\beta=31^\circ$ for the experiments and $\beta=46^\circ$ for the simulations. Pärletun [3] found the crack dividing angel $\beta=26^\circ$ for quasi-static crack growth.

Discussion

The method for estimating the crack widths and crack angels, described earlier was developed to minimise the influence of rigid body motion of the crack surfaces. But it is also associated with some accuracy problems. In some cases, it was difficult to match the middle piece to the correct position, see Fig. 3. The middle piece influences the crack width ratios and even the smallest misfit will influence the ratio. Also, only the surface of the specimens is investigated. What happens in the bulk of the material is not known. The dissolution may differ at the surface, rendering pseudo crack widths that are different from the crack branch width in the bulk. Cutting the specimen in half did not produce better results since the material were damaged to a degree that no cracks were visible.

The comparison with previous work done for quasi-static crack growth must be done with care. Some mcriterion for crack growth and crack branching has been used. In these computations there is no criterion that governs the crack growth, still, the agreement is good, and this supports both results.

It was noticed that the sum of the widths was slightly larger than the width before branching. A reason for this discrepancy could be explained from the cracks geometry. Since the two branches do not grow in parallel to each other, there is an angle between them; there will be an energy contribution to the J-integral. This contribution is not calculated in this study.

The large scatter in the results is hard to minimise. There is an inherent uncertainty in the nature of the stress corrosion phenomenon, which makes predictions hard, so a statistical approach could be preferable. For repeated experiments, even though the cracks are not the same; however, the characteristics are found to be similar.

Conclusion

This paper has presented results from stress corrosion experiments and simulations in polycarbonate with acetone as the dissolving agent. A correlation between the stresses and the amount of dissolved material at the crack tip was found. As the crack branches, the width of the cracks decreases with a factor of approximately 1/2, and the stress intensity factor with a factor approximately $1/\sqrt{2}$, or just above. This supports the theory that the width scales with the stress at the crack tip.

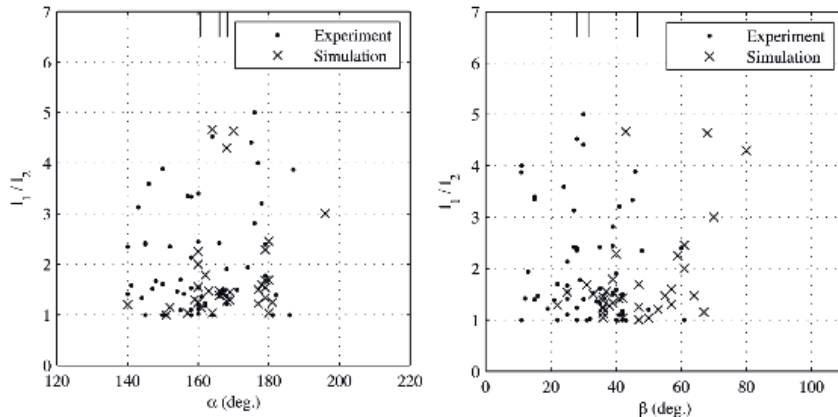


Figure 7. Measurements of the alpha and beta angles individually.

Crack angles were also investigated and it was seen that the experimental crack grows so that average crack path, $\alpha + \beta/2$, is just below 180° and somewhat larger than 180° for the simulations. The crack-dividing angle and the crack kink angle was measured individually. The average values were found to be $\alpha = 161^\circ$ for the experiments and $\alpha = 168^\circ$ for the simulations and $\beta = 31^\circ$ for the experiments and $\beta = 46^\circ$ for the simulations. A comparison with e.g. Pärletun [7] who found a cracks divide angle of $\beta = 26^\circ$ shows a good agreement.

Acknowledgement

I would like to thank Dr. Zoltan Blum at Malmö University for assistance with the polymer chemistry. This investigation was supported by research grants from the Knowledge Foundation (Biofilms – Research centre for Biointerfaces).

Bibliography

- [1] Joseph R. Davis, ASM handbook Vol. 13, Materials Park, 2001, 10th edition, ISBN 0-87170-007-7.
- [2] Russel H. Jones. Stress-corrosion cracking. ASM International 1992, ISBN 0-87170-441-2.
- [3] A. P. Jivkov, P. Stähle. Strain-driven corrosion crack growth - A pilot study of intergranular stress corrosion cracking. Engng. Fracture mech. 2002; 69:2095-2111.
- [4] A. P. Jivkov. Strain-induced passivity breakdown in corrosion crack initiation. Theoretical and Appl. Fracture mech. 2004; 42:43-52.
- [5] B. Sroberg. Cracks and Fracture. Academic press 1999, ISBN 0-12-134130-5.
- [6] L. G. Pärletun. Determination of the growth of branched cracks by numerical methods. Engng. Fracture Mech. 1979;11:343-358.
- [7] V. Vitec. Plane strain stress intensity factors for branched cracks. Int. J. of Fracture 1977;13:481-501.
- [8] X. B. Zhang, S. Ms, N. Recho, J. Li. Bifurcation and propagation of a mixed-mode crack in a ductile material. Engng. Fracture Mech. 2006;73:1925-1939.
- [9] S. Suresh, C. F. Shih. Plastic near-tip fields for branched cracks. Int. J. of Fracture 1986;30:237-259.
- [10] P. S. Theocaris. Complex stress-intensity factors at bifurcated cracks. J. of Phys. solids 1972; 20:265-279.
- [11] P. S. Theocaris. Asymmetric Branching of Cracks. J. of Appl. Mech. 1977:611-618.
- [12] P. S. Theocaris, N. P. Andrianopoulos, S. K. Kourkoulis. Crack branching: A twin-crack model based on macroscopic energy Fracture criteria. Engng. Fracture Mech. 1989;34:1097-1107.
- [13] C. S. Carter. Stress corrosion crack branching in high-strength steels. Engng. Fracture Mechanichs 1971;3:1-13.
- [14] P. Stähle, C. Bjerkén, A. P. Jivkov. On dissolution driven crack growth. Int. J. of Solids Struct. 2007;44:1880-1890.
- [15] I. Ghorbel. F. ThomINETTE, P. SpITERI, J. Verdu. Hydrolytic aging of polycarbonate, II. Hydrolysis kinetics, effect of static stresses. J. of Appl. Polymer Sci. 1995;55:173-179.
- [16] Kitagawa H, Tuuki R. Crack-morphological aspects in fracture mechanics. Fracture Mechanics 1975;7:515-529.